THE JOURNAL OF BIOLOGICAL CHEMISTRY VOL. 282, NO. 35, pp. 25893–25902, August 31, 2007

The Tandem β-Zipper Model Defines High Affinity Fibronectin-binding Repeats within *Staphylococcus aureus* FnBPA*[S]

Received for publication, April 11, 2007, and in revised form, June 15, 2007 Published, JBC Papers in Press, July 2, 2007, DOI 10.1074/jbc.M703063200

Nicola A. G. Meenan[‡], Livia Visai[§¶], Viviana Valtulina[§], Ulrich Schwarz-Linek[‖], Nicole C. Norris[‡], Sivashankarappa Gurusiddappa[**], Magnus Höök[1], Pietro Speziale[§2], and Jennifer R. Potts[‡ ‡‡3]**

From the [‡]Department of Biology, University of York, P.O. Box 373, York YO10 5YW, United Kingdom, the [§]Department of Biochemistry, University of Pavia, Viale Taramelli 3/B 27100 Pavia, Italy, [¶]Centro di Ingegneria Tissutale, University of Pavia, Viale Taramelli 3/B 27100 Pavia, Italy, the [‖]Centre for Biomolecular Sciences, University of St. Andrews, North Haugh, St. Andrews, Fife KY16 9ST, United Kingdom, the [**]Center for Extracellular Matrix Biology, Institute of Biosciences and Technology, Texas A & M University System Health Science Center, Houston, Texas 77030-3303, and the [‡‡]Department of Chemistry, University of York, York YO10 5DD, United Kingdom

Binding of the fibronectin-binding protein FnBPA from *Staphylococcus aureus* to the human protein fibronectin has previously been implicated in the development of infective endocarditis, specifically in the processes of platelet activation and invasion of the endothelium. We recently proposed a model for binding of fibronectin to FnBPA in which the bacterial protein contains 11 potential binding sites (FnBPA-1 to FnBPA-11), each composed of motifs that bind to consecutive fibronectin type 1 modules in the N-terminal domain of fibronectin. Here we show that six of the 11 sites bind with dissociation constants in the nanomolar range; other sites bind more weakly. The high affinity binding sites include FnBPA-1, the sequence of which had previously been thought to be encompassed by the fibrinogen-binding A domain of FnBPA. Both the number and sequence conservation of the type-1 module binding motifs appears to be important for high affinity binding. The *in vivo* relevance of the *in vitro* binding studies is confirmed by the presence of antibodies in patients with *S. aureus* infections that specifically recognize complexes of these six high affinity repeats with fibronectin.

Staphylococcus aureus is one of the most important bacterial pathogens to affect humans. Clinical manifestations of infection range from superficial skin infections (1) to life-threatening conditions, such as endocarditis (2, 3) and difficult to treat infections of the bones and joints (4, 5). The increasing virulence and antibiotic resistance exhibited by this major source of both community and hospital-acquired infection presents an urgent challenge. Furthering our understanding of the mechanism by which staphylococcal pathogenesis occurs is thus imperative for the development of novel therapeutic and preventative strategies.

Since attachment to host tissue is a critical early step in infection, one particular group of targets for intervention is the microbial surface components recognizing adhesive matrix molecules (MSCRAMM)[4] family of surface-expressed adhesins (6, 7). These proteins exploit extracellular matrix proteins, such as fibronectin (Fn), using them as a bridge between the bacterial cell surface and host cell receptors that effect downstream signaling (8, 9). Although classically regarded as an exclusively extracellular pathogen, *S. aureus* has been shown to adhere to and invade several host cell types (10–14), and the Fn-binding subfamily of MSCRAMMs (FnBPs) appears to be involved in this process (15). There is an emerging view that *S. aureus* can exist intracellularly, hijacking and invading host cells to establish persistence (16). Conceivably, this mechanism could facilitate rapid and effective bloodstream dissemination while allowing the bacterium to evade antibiotics and host immune surveillance, an apposite theory given the prevalence of bacterial metastasis (3) and infection relapse in staphylococcal disease (17).

Fn is a large glycoprotein present in a soluble form in human plasma and other body fluids and in an insoluble form in the extracellular matrix. Its principal functions include cellular adhesion, differentiation, and tissue repair. The protein has a modular structure and is composed of type 1, type 2, and type 3 (F1, F2, and F3) modules. FnBPs from *S. aureus*, *Streptococcus pyogenes*, *Streptococcus dysgalactiae* and *Borrelia burgdorferi*

* This work was supported by the Italian Ministero dell'Istruzione, dell'Università e della Ricerca, IDEE PROGETTUALI (Grandi Programmi Strategici, Decreto Ministeriale 24695, Protocollo RBIPO6FH7J) (to L. V.), Fondazione CARIPLO (2003 1640/10.8485), Fondo di Ateneo per la Ricerca (Pavia, Italy), and PRIN 2001 (Prot. 20011061977_004) (to P. S.). The costs of publication of this article were defrayed in part by the payment of page charges. This article must therefore be hereby marked "*advertisement*" in accordance with 18 U.S.C. Section 1734 solely to indicate this fact.

[S] The on-line version of this article (available at http://www.jbc.org) contains supplemental Tables 1 and 2.

[1] Supported by National Institutes of Health Grant AI020624.

[2] To whom correspondence may be addressed. Tel.: 39-0382-987787; Fax: 39-0382-423108; E-mail: pspeziale@unipv.it.

[3] Supported by the British Heart Foundation and the Wellcome Trust. To whom correspondence may be addressed: Dept. of Biology, University of York, P.O. Box 373, York YO10 5YW, United Kingdom. Tel.: 44-1904-328679; Fax: 44-1904-328825; E-mail: jp516@york.ac.uk.

[4] The abbreviations used are: MSCRAMM, microbial surface components recognizing adhesive matrix molecules; LIBS, ligand-induced binding sites; Fn, fibronectin; ITC, isothermal titration calorimetry; FnBR, fibronectin-binding repeat; NTD, N-terminal domain; Fib1, proteolytic fragment encompassing the N-terminal domain of fibronectin; HRP, horseradish peroxidase; Fg, fibrinogen; mAb, monoclonal antibody; FnBP, fibronectin-binding protein; LB, Luria-Bertani.

(18–21) all bind the N-terminal domain (NTD) of Fn, which is composed of a string of five F1 modules (7, 22–24).

S. aureus contains two principal FnBPs, FnBPA and FnBPB, each having similar organization and gene structure. Two separate analyses of clinical isolates (25, 26) have shown all to contain at least one *fnbp* gene, with many (37 and 77%, respectively) containing two. Furthermore, FnBPs participate in chronic and deep seated bacterial infection via adhesion to surgical implants (27). Antibiotic-resistant strains appear to show similar distribution levels, with 91% of methicillin-resistant samples ($n = 46$) in one study testing positive for both genes (28). Common features of FnBPA and FnBPB (Fig. 1*A*), include a hydrophobic cell wall anchor, an LP*X*TG motif that has been shown to be crucial for host cell attachment (29), and an unstructured region with Fn binding activity. FnBPA also possesses fibrinogen (Fg) (30) and tropoelastin (31) binding capacity, mediated by the N-terminal A domain region. In both FnBPA and FnBPB, this region also binds elastin (32).

In FnBPA, the Fn binding activity was initially identified in a stretch of repetitive sequence in the C-terminal "D-region" (18). More recently, we have proposed a Fn-binding repeat (FnBR) classification based on structural data for a complex between two F1 modules of Fn and a peptide from a streptococcal FnBP (33). Upon binding, the bacterial peptide forms a β-strand that aligns antiparallel to an existing sheet in each of the Fn F1 modules. In this β-zipper model, sequential F1 modules in the NTD of human Fn (Fig. 1*B*) engage specific motifs in an FnBR. Thus, the mosaic structure of the NTD (Fig. 1*B*) is mirrored within each FnBR. The mechanism of interaction requires that bacterial F1-binding motifs be presented to the NTD in the same sequence as the F1 modules in order for high affinity binding to occur. This new classification extends the number of potential Fn-binding sites in FnBPA to 11.

The main aim of this work is to address three key aspects of the FnBPA-Fn interaction that are predicted by the new classification of FnBRs. First, using a variety of assays, we demonstrate Fn binding for nine of the 11 repeats defined by our model. Second, we show that high affinity sites for Fn occur outside the traditionally defined D-region. Third, we show that a specific order and composition of bacterial F1-binding motifs appears to be required for high affinity interactions of FnBRs with Fn. In addition, it is shown that although isolated FnBRs are recognized weakly by antibodies, upon complexation with Fn, ligand-induced binding site (LIBS) epitopes are formed that are recognized by both monoclonal antibodies (mAbs) and by sera from patients with staphylococcal infections. Collectively, these results strongly support both the idea that *S. aureus* engages Fn through a tandem β-zipper mechanism and the reclassification of FnBR boundaries.

EXPERIMENTAL PROCEDURES

Bacterial Strains, Plasmids, and Culture Conditions

Escherichia coli strain BL21 was used as a host, and pGEX-2T, pGEX-5X, or pGEX-6P2 (GE Healthcare) was used as vector for cloning and expressing recombinant FnBRs from FnBPA. *S. aureus* strain Newman was obtained from Prof. T. J. Foster (Trinity College, Dublin, Ireland). *E. coli* strains were grown in LB broth or on LB agar at 37 °C with appropriate antibiotics. Staphylococci were grown in brain heart infusion (Difco) broth or on brain heart infusion agar at 37 °C overnight with constant shaking.

Routine DNA Manipulation and Transformation of E. coli

DNA preparation, purification, restriction digestion, agarose gel electrophoresis, and ligation were performed using standard methods (34) or following the manufacturer's instructions unless otherwise stated. All enzymes were purchased from New England BioLabs Inc. Plasmid DNA was isolated using the QIAprep Spin Miniprep kit (Qiagen). Routine preparation of *E. coli* competent cells and transformation of DNA into *E. coli* were performed by a one-step procedure (35).

Cloning of FnBR Constructs

S. aureus genomic DNA, isolated as previously described (36), was used as template for all PCR reactions except those amplifying DNA for constructs of FnBPA-4 and FnBPA-5 used in isothermal titration calorimetry (ITC) experiments (supplemental Table 1). In this case, a pQE vector (Qiagen) encoding full-length FnBPA was used as template. In all cases, oligonucleotide primers were designed to encode BamHI (5′-end) and EcoRI site (3′-end) restriction sites (supplemental Table 1). PCR products were digested with BamHI and EcoRI, purified, and ligated to BamHI- and EcoRI-digested and dephosphorylated pGEX-2T (for cloning of FnBPA-1 and -11), pGEX-5X (for cloning of FnBPA-2, -3, -4, -5, -6, -7, -8, -9, and -10), and pGEX-6P2 (for cloning of FnBPA-4 and FnBPA-5 constructs used in ITC) (supplemental Table 1). The ligation mixture was transformed into *E. coli* BL21, and the cells were incubated on LB agar plates (100 μg/ml ampicillin) (Sigma) at 37 °C to select for transformants. Insertions were confirmed by DNA sequencing.

Expression and Purification of Recombinant FnBRs

FnBRs were expressed as glutathione *S*-transferase (GST) fusion proteins. *E. coli* BL21 transformed with a particular pGEX-FnBR construct was selected on LB agar (100 μg/ml ampicillin). An overnight culture of transformant was diluted 1:100 in LB medium and grown at 37 °C, with shaking (225 rpm), until A_{600} nm reached 0.5–0.6. Expression was induced by adding isopropyl-β-thiogalactopyranoside (Melford Laboratories) to a final concentration of 0.3 mM. Bacteria were harvested by centrifugation and lysed by passage through a French press. The cell debris was removed by centrifugation (20,000 × *g*), and filtered supernatant (0.45-μm membrane) was applied to a 5-ml glutathione-Sepharose-4B® column (GE Healthcare). Fusion protein was eluted with five column volumes of 10 mM reduced glutathione GSH (Sigma) in 50 mM Tris-HCl, pH 8.0. For solid phase binding studies, fractions corresponding to each recombinant protein, as determined by SDS-PAGE were pooled and extensively dialyzed against phosphate-buffered saline (PBS; 140 mM NaCl, 2.7 mM KCl, 10.0 mM Na_2PO_4, 1.8 mM KH_2PO_4, pH 7.4). A single band of the expected molecular weight was observed for each of the different FnBR GST fusions on SDS-PAGE. Protein concentrations were determined using the absorbance at 280 nm or using a BCA (bicinchonic acid) protein assay kit (Pierce).

TABLE 1

Thermodynamic parameters for the interaction of Fib1 with FnBRs from FnBPA

FnBPA residues (Swiss-Prot entry P14738) encoded by each construct are indicated in parentheses. The data were obtained using ITC at physiological salt strength, pH 7.4, 25 °C. The binding of the D-repeat peptides to Fib1 was too weak to be determined under these conditions.

	FnBPA residues	Potential interaction motifs (in order, from N terminus)	[Fib1]	[FnBR]	ΔH	ΔS	K_D	n
			μM	μM	*kcal mol*$^{-1}$	*cal mol*$^{-1}$ *K*$^{-1}$	nM	
FnBPA-1	512–550	^{5}F1-^{4}F1-^{3}F1-^{2}F1	4.5	51	−26.0	−49.1	4.8 ± 0.6	0.84
FnBPA-4	610–636	^{4}F1-^{3}F1-^{2}F1	4.8	48	−28.9	−60.4	10.5 ± 0.9	0.37
FnBPA-5	637–672	^{5}F1-^{4}F1-^{3}F1-^{2}F1	5.0	60	−17.0	−23.4	44.2 ± 9.7	0.91
FnBPA-8	733–762	^{4}F1-^{3}F1-^{2}F1	4.7	50	−19.5	−40.0	~3000[a]	0.76
FnBPA-9	763–800	^{5}F1-^{4}F1-^{3}F1-^{2}F1	4.8	36	−28.0	−56.7	7.3 ± 0.4	0.99
FnBPA-10	801–838	^{5}F1-^{4}F1-^{3}F1-^{2}F1	5.3	48	−24.4	−46.5	19.5 ± 1.1	0.98
FnBPA-11	839–874	^{5}F1-^{4}F1-^{3}F1-^{2}F1	5.8	79	−28.4	NF	<1.0[b]	1.01
D1	745–782	*^{3}F1-^{2}F1-*^{5}F1-^{4}F1	5.0	53	(exothermic)	NF	NF	NF
D2	783–820	*^{3}F1-^{2}F1-*^{5}F1-^{4}F1	4.3	43	(exothermic)	NF	NF	NF

[a] The shape of the curve precludes a reliable fit to these data.
[b] The steepness of the binding isotherm transition precludes a reliable fit of these data. Binding was also analyzed at 37 °C, but again the transition was too steep to fit reliably (NF, not fitted). Italic type indicates that the F1-binding motifs in D1 and D2 are in a different sequential order than in the FnBRs.

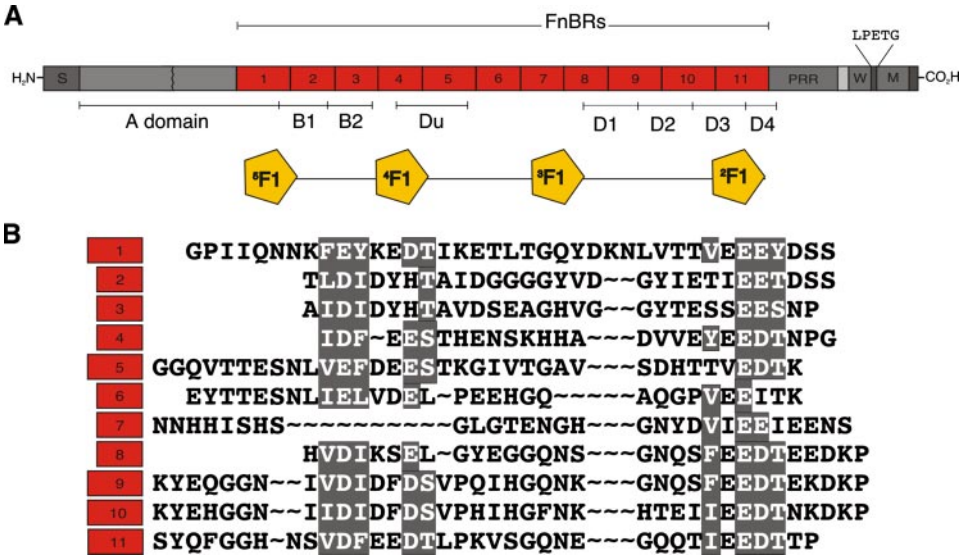

FIGURE 1. **FnBPA from *S. aureus* contains 11 Fn-binding sites predicted to bind Fn with varying affinity.** *A*, schematic of FnBPA from *S. aureus* showing the approximate position of the 11 predicted FnBRs (FnBPA1 to -11) within the bacterial protein sequence (33). Also shown are the locations of signal peptide (*S*), Fg-binding region (*A*), proline-rich repeats (*PRR*), cell wall-spanning sequence (*W*), membrane-spanning region (*M*), and the previously defined Fn-binding regions (*D1–D4*, *B1*, *B2*, and *Du*). *B*, the amino acid sequences of the 11 FnBRs. Conserved residues are shown in *white text*. The putative binding sites (within $^{2-5}$F1 of Fn) of motifs within each repeat are indicated *above* the sequence alignment.

For ITC, GST fusion proteins were cleaved by thrombin (pGEX-2T series; Sigma), Factor Xa (New England Biolabs; pGEX-5X series), or 3C proteases (pGEX-6P series; GE Healthcare). After enzymatic cleavage, the residues GS, GIP, and GPLGS, respectively, were retained at the N terminus of the FnBR. FnBRs further purified by reverse-phase high performance liquid chromatography as previously described (37) were subsequently lyophilized, and molecular weights were confirmed by electrospray-ionization mass spectrometry. Concentrations were determined from absorbance at 280 nm by weighing freeze-dried material or from amino acid analysis.

Preparation of Fn and Fn Fragments and Peptide Synthesis

Human Fn was prepared as previously reported (38). For solid-phase binding studies, the N-terminal Fn fragment (Fib1) was isolated using the procedure described by Zardi *et al.* (39), whereas for ITC, Fib1 was obtained commercially (Sigma). Peptides D1, D2, and D3 were synthesized and purified as previously described (40).

Monoclonal Antibody Preparation

mAbs directed toward full-length FnBPA or recombinant GST-D1–D3 were raised as previously described (41, 42). Full-length FnBPA was purified from *S. aureus* Newman as described previously (43). Plasmid pGEXD1–3, for expression in *E. coli* of the GST fusion protein GST-D1–D3, has been described elsewhere (44).

Isotyping of the mAbs was performed using a Mouse-Typer sub-isotyping kit (Zymed Laboratories, San Francisco, CA). Four clones producing mAbs to full-length FnBPA (1F9 (IgG_{2b-k}), 5G3 (IgG_{1-k}), and 6B7 (IgG_{2b-k})) or D1–D3 (7D4 (IgG_{1-k})) were subcloned and grown to high cell density. The antibodies were purified by using ammonium sulfate precipitation of the supernatant, followed by affinity chromatography on Protein A/G-Sepharose columns according to the manufacturer's protocol (GE Healthcare). No cross-reactivity of the produced mAbs toward Fn or Fn fragments was observed either in an enzyme-linked immunosorbent assay or Western blot.

An anti-GST mAb 10G7 (IgG_{1-k}) was produced by immunization of mice with the purified GST as described above. Mouse anti-Fib1 mAb 843 was kindly provided by L. Zardi (Cell Biology Laboratory, Istituto Nazionale per la Ricerca sul Cancro, Genoa, Italy). Anti-human Fn polyclonal antibody was obtained by immunizing a rabbit with a purified preparation of human Fn.

Solid-phase Binding Assay

Fn and Fib1 Binding to FnBRs of FnBPA—Microtiter wells were coated overnight at 4 °C with 100 μl of 5 μg/ml FnBPA-1,

-2, -3, -4, -5, -6, -7, -8, -9, -10, and -11 in fusion with GST or with GST alone in coating buffer (50 mM sodium carbonate, pH 9.5). After washing with PBST (PBS containing 0.1% (v/v) Tween 20), the wells were blocked for 1 h at 22 °C with 200 μl of PBS containing 2% (w/v) BSA. Subsequently, 100 μl of either Fn (5.25 μg/ml) or Fib1 (0.75 μg/ml) was added to the wells before incubation at 22 °C (1 h). Wells were washed with PBST and incubated with 100 μl of rabbit anti-human Fn polyclonal antibody (10 μg/ml) or mouse anti-Fib1 mAb 843 (10 μg/ml) for 90 min at 22 °C. Binding of anti-Fn or anti-Fib1 antibodies to the wells was detected by incubating the plates with 100 μl of horseradish peroxidase (HRP)-conjugated goat anti-rabbit IgG or of HRP-conjugated rabbit anti-mouse IgG (1:1000 dilution; DakoCytomation, Glostrup, Denmark), respectively, for 1 h at 22 °C. The binding of the secondary antibody was quantified by adding the substrate *o*-phenylenediamine dihydrochloride and measuring the resulting absorbance at 490 nm in a microplate reader (Bio-Rad). The coating efficiency with each FnBR-GST was verified by incubating the wells with an anti-GST mouse mAb 10G7; in the assay conditions used, all of the recombinant FnBRs showed very similar reactivity with the anti-GST antibody. The saturability of the binding was determined in an enzyme-linked immunosorbent assay by incubating the FnBR-coated wells with increasing concentrations (0–120 nM) of Fib1 and with spectrophotometric detection of Fib1 as described above.

Binding of mAbs to FnBRs—Microtiter wells coated with each of the 11 FnBRs of FnBPA (5 μg/ml) were preincubated with PBS alone or with Fn (5.25 μg/ml) or Fib1 (0.75 μg/ml) in PBS. After washing with PBST, 100 μl of the mAbs 1F9, 5G3, 6B7, or 7D4 (2.5 μg/ml) was added to the wells before incubation at 22 °C for 1 h. Bound mAb was detected by incubation with a 1:1000 dilution of HRP-conjugated rabbit anti-mouse polyclonal antibodies. The monoclonal antibody 7E11 produced against FnbB (42) was used as a negative control.

Identification of LIBS Antibodies in Human Sera of Patients with Staphylococcal Infections—Serum antibodies from patients with staphylococcal endocarditis were purified as previously described (45). Diagnosis of infection was made on the basis of clinical, laboratory, and echocardiographic data, and the clinical characteristics of the patients used in this study are reported in supplemental Table 2. To assess the binding of purified IgG (from patient serum) to the 11 FnBRs of FnBPA, microtiter wells were coated with the individual repeats (5 μg/ml) and then incubated without or with Fn (20 μg/ml) for 90 min at 22 °C. After washing, 1 μg of each antibody preparation was added to the wells. Bound antibody was detected by incubation for 1 h at 37 °C with HRP-conjugated rabbit anti-human polyclonal antibodies (1:2000 dilution; Dako Cytomation). IgG from healthy donors was used as a control. To exclude the possibility that patient IgG could react with Fn alone, microtiter plates were coated with 1 μg of human Fn and then tested with 1 μg of each antibody preparation. Under these conditions, no reactivity of antibodies to Fn was detected.

ITC Experiments

Calorimetry experiments were carried out using a VP-ITC instrument (MicroCal Inc., Northampton, MA). In a typical

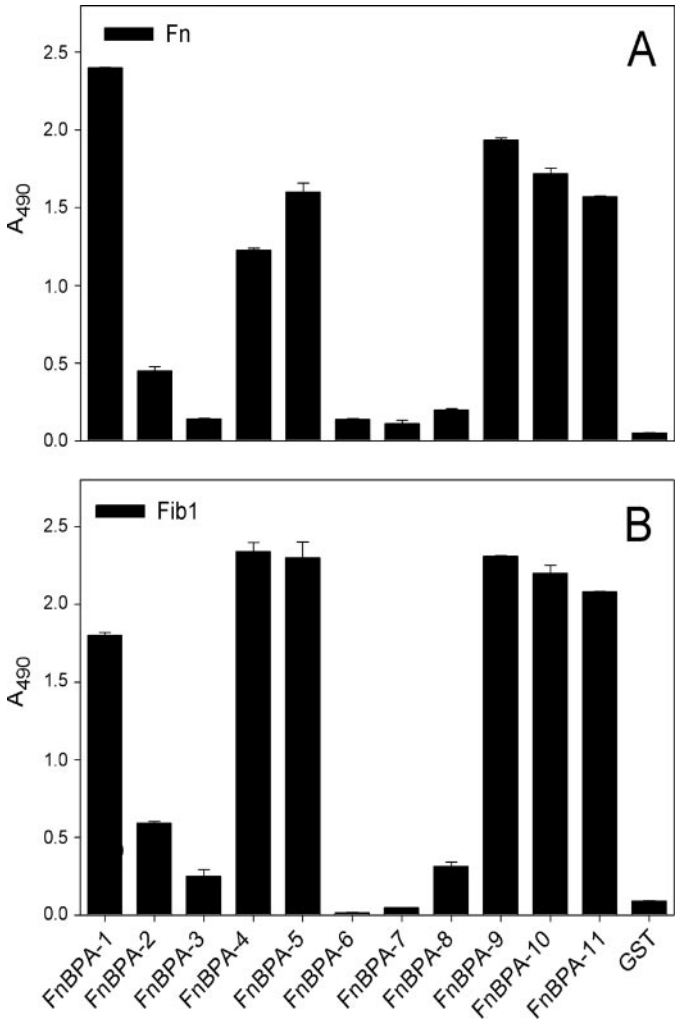

FIGURE 2. **Binding of Fn or Fib1 to the 11 predicted FnBRs.** Recombinant FnBRs in fusion with GST were immobilized onto microtiter wells (0.5 μg in 100 μl) and probed with 100 μl of 5.25 μg/ml of Fn (*A*) or 0.75 μg/ml Fib1 (*B*). After washing, the wells were incubated with 1 μg of a rabbit anti-Fn polyclonal antibody (*A*) or a mouse anti-Fib1 mAb 843 (*B*). Bound antibody was detected by incubation with either goat anti-rabbit (*A*) or rabbit anti-mouse (*B*) secondary HRP-conjugated antibody as described under "Experimental Procedures." Values are the mean ± S.D. of triplicate assays.

experiment, the calorimeter cell contained 1.4 ml of Fib1, and the syringe contained 295 μl of concentrated FnBR (Table 1). The concentration of protein in the syringe was typically 10–15 times that in the cell, whereas the cell concentration was chosen according to a predicted *c* value of 100–1000, where $c = [\text{macromolecule}]/(\text{predicted})\ K_D$ (46). Experiments were carried out in PBS, pH 7.4. Both cell and syringe solutions were filtered through 0.22-μm membranes and degassed at 20 °C for 10 min before use.

The titrations were performed as follows. A single preliminary injection of 2 μl of FnBR solution was followed by 20–40 injections (5–7 μl), delivered at an injection speed of 0.5 μl s^{-1}. Injections were spaced over 4–5-min intervals at a stirring speed of 310 rpm. For all titrations, other than those involving D1 and D2, the shape of the binding isotherm allowed heats of dilution to be assessed by continuing peptide injections beyond saturation and obtaining an average value over several post-

transition injection points. The averaged heat of dilution was then subtracted from the main experiment. For FnBPA-8, D1, and D2 a separate heat of dilution control experiment where equivalent volumes of peptide were injected into buffer was performed. This ruled out the possibility of large heats of dilution masking weak binding. Raw titration data were integrated and fit to a one-site model of binding using MicroCal Origin version 7.0.

RESULTS

Repeats throughout the FnBPA Array Bind NTD of Fn with High Affinity—Previous analyses of staphylococcus-Fn interactions suggested that high affinity Fn binding is limited to the C-terminal D region (18, 44, 47). Subsequent studies established additional discrete Fn binding activity within the C (or Du), B domains (11, 47, 48), and A domain (49). Previously, we suggested that FnBPA in fact contains 11 contiguous FnBRs and that these would bind Fn with varying affinities largely dependent on the number of proposed F1 module binding motifs in the FnBR and on the presence of conserved residues.

Fig. 1 shows a sequence alignment of predicted FnBRs from *S. aureus* FnBPA, based on our tandem β-zipper model for binding to Fn (33). The sequence alignment suggests that the FnBRs FnBPA-1, -5, -6, -9, -10, and -11 contain motifs that will bind four sequential modules ($^{2-5}$F1) in the NTD of Fn. FnBPA-2, -3, -4, and -8, lack the putative ^{5}F1-binding motif, so they are only predicted to bind three F1 modules ($^{2-4}$F1) and therefore might be expected to bind with lower affinity. FnBPA-7 lacks the ^{4}F1-binding motif and therefore might only be expected to bind ^{2}F1^{3}F1. Additionally, we note differences in conservation of amino acids in the ^{2}F1- and ^{4}F1-binding motifs, with only five FnBRs, FnBPA-1, -4, -9, -10, and -11, containing a particular set of nine conserved residues (*highlighted* in *gray* in Fig. 1*B*).

Fig. 2 shows the results of a solid-phase (enzyme-linked immunosorbent assay) binding assay in which the affinities of the 11 predicted Fn-binding repeats for intact Fn and Fib1 were compared. This experiment identified six potential high affinity binding repeats (FnBPA-1, -4, -5, -9, -10, -11). The similarity of the results when Fn or Fib1 was used as a ligand confirms the NTD of Fn as the binding site for all FnBRs except for FnBRs 6 and 7, for which no significant binding to Fib1 was detected in Fig. 2*B*. However, this is likely to be a result of the sensitivity of the assay, since binding of FnBPA-7 to Fib1 is demonstrated in Fig. 3. Dose-response experiments showed that Fib1 bound to the indicated FnBRs in a saturable manner and confirmed that FnBPA-1, -5, and -9 bind with higher affinity (Fig. 3*A*) to Fib-1 than FnBPA-2, -3, and -7 (Fig. 3*B*).

The ITC experiments shown in Fig. 4 and summarized in Table 1 show that the FnBRs that were identified as high affinity binders in the solid phase assay (Fig. 1) bind Fib1 with dissociation constants (K_D) of between 1.0 and 44.2 nM at physiological ionic strength. FnBPA-8, which bound Fib1 weakly in the solid-phase binding assay, also binds weakly under the ITC experimental conditions. As mentioned above, with the exception of

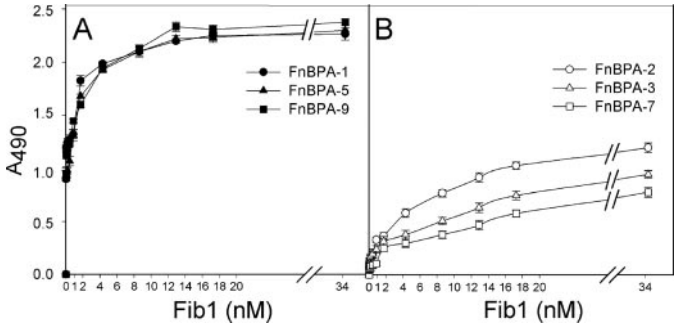

FIGURE 3. **Concentration-dependent binding of Fib1 to high and low affinity FnBRs from FnBPA.** Microtiter wells coated with 0.5 μg of FnBPA-1, -5, or -9 (*A*) or FnBPA-2, -3, or -7 (*B*) were incubated with increasing concentrations of Fib1. Then 1 μg of a mouse anti-Fib1 mAb 843 was added to the wells. After washing, bound antibody was detected by incubating with a rabbit anti-mouse HRP-conjugated antibody as described under "Experimental Procedures." In cases where S.D. is not shown, bars do not exceed the size of the *symbols*. In *A*, the *three symbols* overlap at the lowest Fib1 concentration.

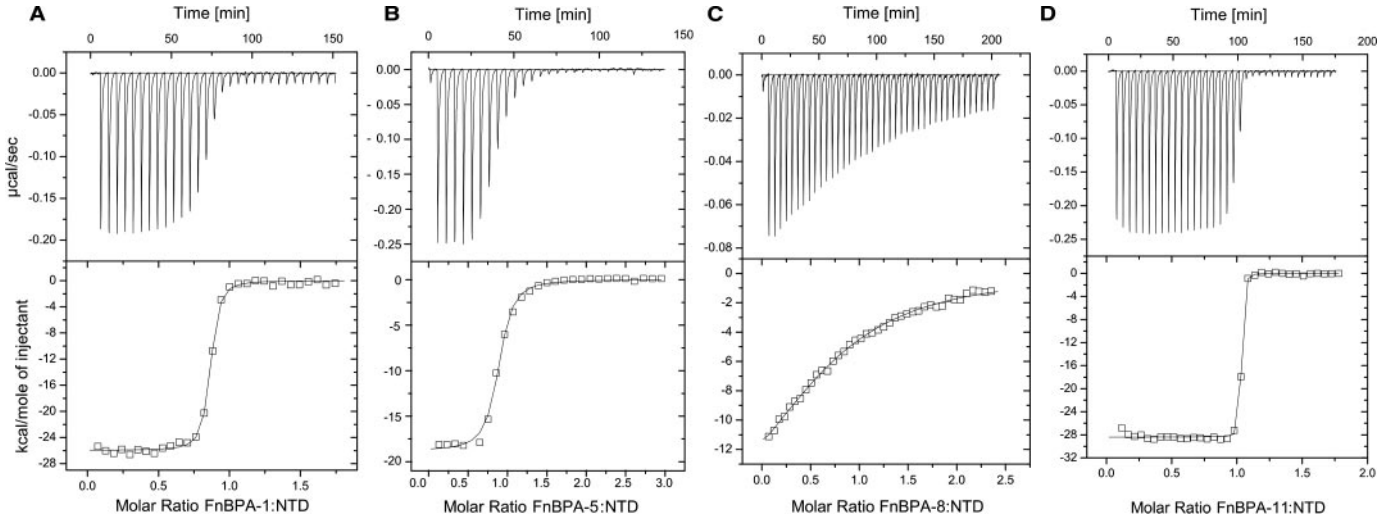

FIGURE 4. **ITC for determination of K_D values.** Shown are binding isotherms for the interaction of Fib1 with FnBPA-1 (*A*), FnBPA-5 (*B*), FnBPA-8 (*C*), or FnBPA-11 (*D*). The *top panels* show heat differences upon injection of FnBR, and the *lower panels* show integrated heats of injection (□) and the best fit (*solid line*) to a single site binding model using Microcal Origin. Thermodynamic parameters for these experiments are summarized in Table 1.

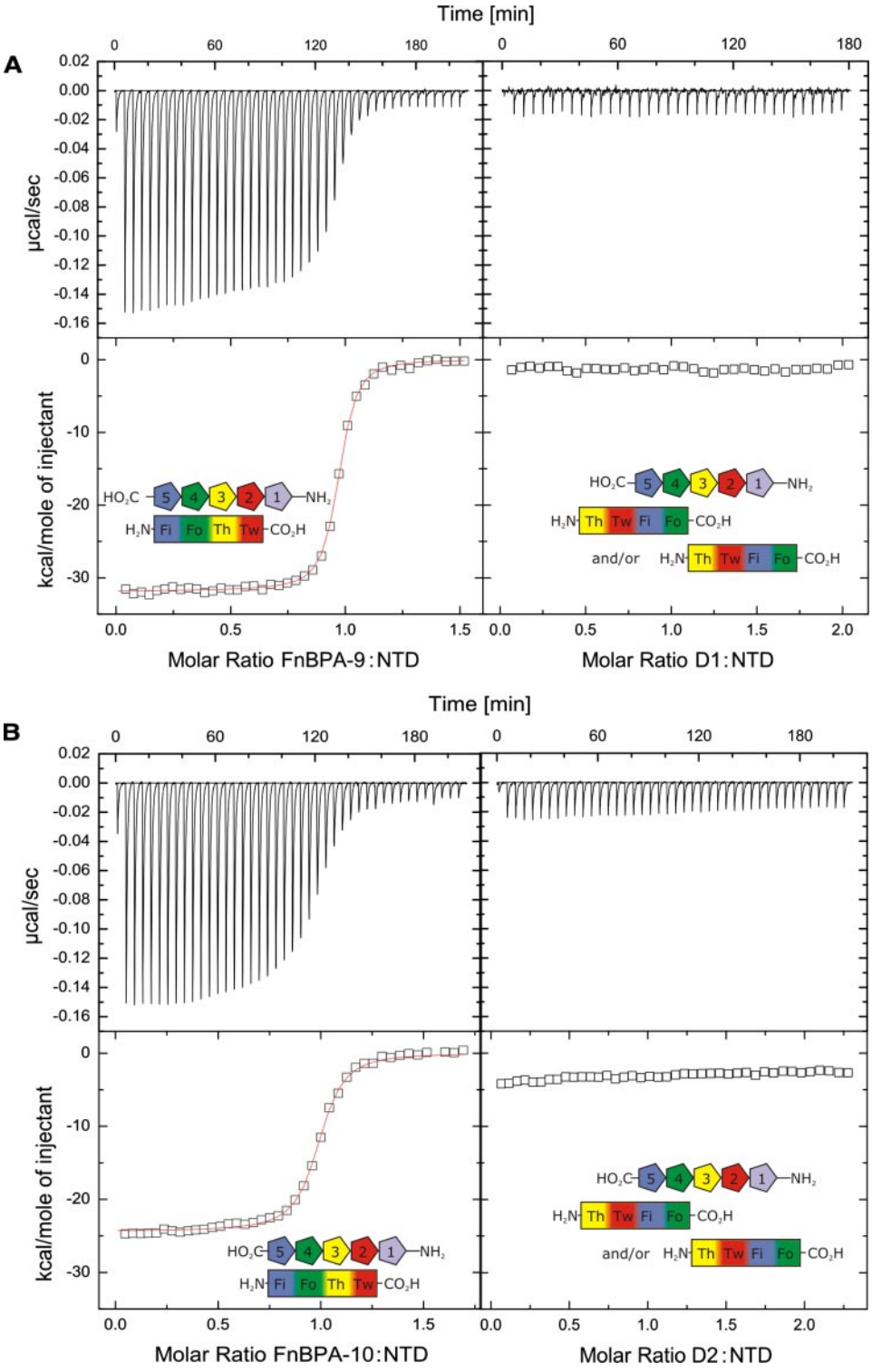

FIGURE 5. **Binding isotherms for the interaction of Fib1 with FnBRs and D-repeats in FnBPA.** Shown is binding of Fib1 (containing the NTD of Fn) to FnBPA-9 (*left*, match binding) and D1 (*right*, mismatch binding) (*A*) and FnBPA-10 (*left*, match binding) and D2 (*right*, mismatch binding) (*B*). Likely interaction modes are indicated in each *panel*. Thermodynamic parameters for these experiments are summarized in Table 1.

FnBPA-4, all of the high affinity FnBRs contain four sequential F1-binding motifs. The relative affinities of Fib-1 binding of FnBPA-4 (10.5 nM) and FnBPA-5 (44.2 nM) are not consistent with affinity being dependent only on the number of proposed F1-binding motifs. FnBPA-4 contains only three predicted F1-binding motifs and yet still binds Fn and Fib-1 with relatively high affinity. FnBPA-5, however, has four F1-binding motifs but lacks one of the nine residues conserved in the other high affinity motifs (Fig. 1). In all FnBRs that bind with high affinity, the (D/E) (T/S) sequence in the ^{2}F1- and ^{4}F1-binding motifs is conserved (33). This is also in accord with our previously published data for Fn binding of SfbI of *S. pyogenes*. Binding of isolated ^{3}F1- and ^{5}F1-binding motifs was too weak to be detected, but they clearly bound their respective modules when in the context of longer constructs (37). In summary, the data in Figs. 1–4 and Table 1 show that FnBPA contains six high affinity sites for interaction with Fn and that weaker Fn binding is observed for other FnBRs.

Match and Mismatch Binding—For a high affinity interaction with Fib-1, FnBRs must contain F1 motifs in the correct sequential order. In order to compare the affinities of binding of the FnBRs to Fib1 with the previously described D-region repeats, the affinities of the FnBPA-9/Fib1 and FnBPA-10/Fib1 interactions were compared with those of D1 and D2 with Fib1 (Fig. 5, *A* and *B*) (18). According to the β-zipper model, each of these four peptides (FnBPA-9, FnBPA-10, D1, and D2) contains four potential F1-interacting motifs; however, it is only within FnBPA-9 and FnBPA-10 that these are arranged in the correct order to bind four F1 modules ($^{2-5}$F1) in a single Fn (or Fib1) monomer. Although FnBPA-9 and FnBPA-10 interact with Fib1 with K_D values of 7.3 and 19.5 nM (Fig. 5), D1 and D2 show virtually no activity under the same conditions (Fig. 5), consistent with K_D values in the micromolar range, as had previously been reported (44). We used a similar experiment to demonstrate the importance of the chosen repeat boundaries in SfbI from *S. pyogenes* (37). Our observations thus support not only the existence of F1 module-binding motifs within each FnBR but also the requirement that they be arranged in consecutive order for high affinity binding to Fn.

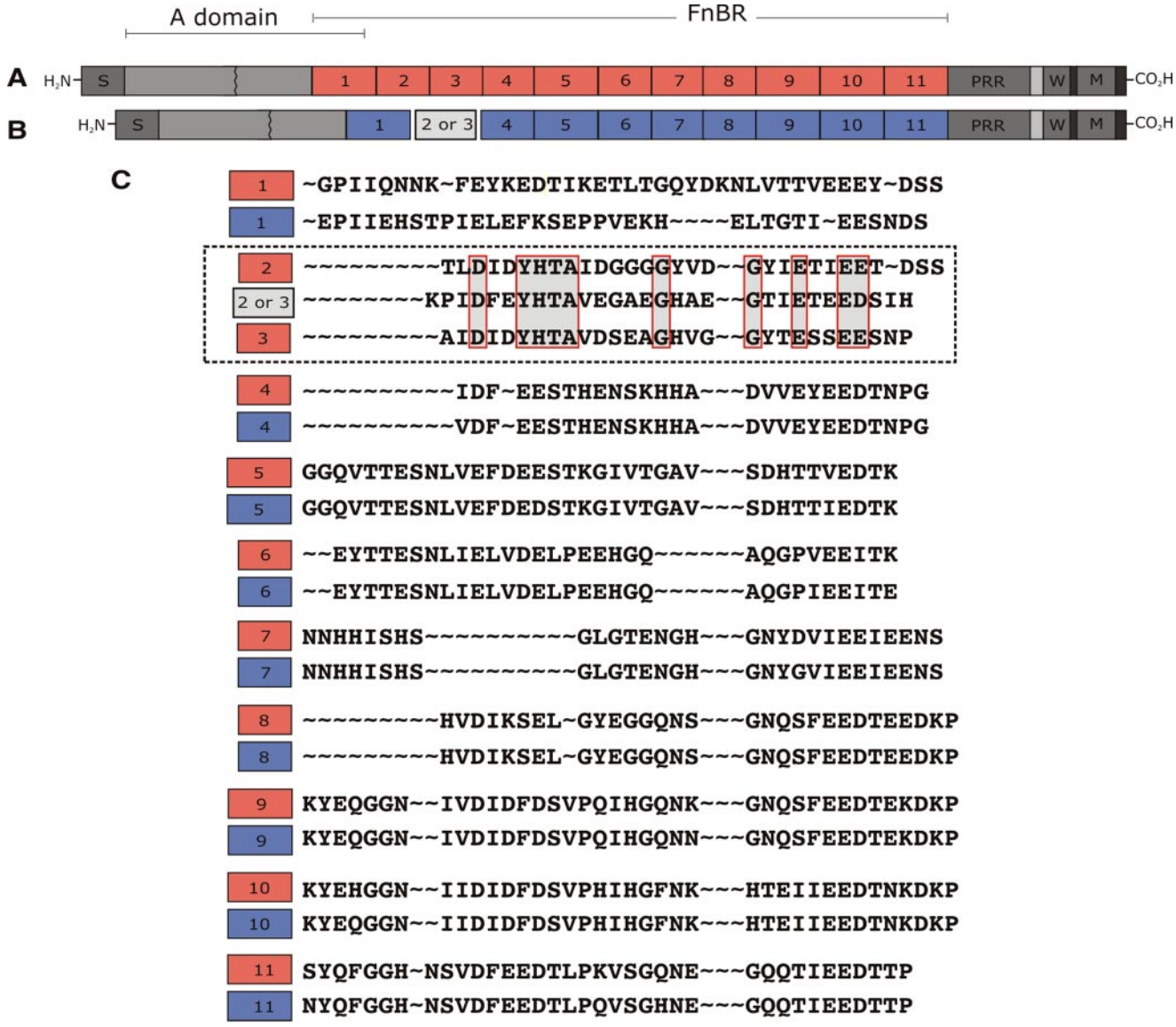

FIGURE 6. **Alignment of FnBPA and FnBPB sequences.** The sequence of FnBPB (Swiss-Prot entry Q53682) was aligned with that of FnBPA (P14738) repeats as defined by the β-zipper model using JPRED (available on the World Wide Web) with some manual editing of the alignment. The alignment shows that FnBPB is missing an FnBR (FnBPB-2 or FnBPB-3). The *red boxes* show residues that are identical between FnBPA-2 and FnBPA-3 and the second FnBR of FnBPB. We note that all high affinity Fn-binding sites in FnBPA are retained in FnBPB.

FnBRs in FnBPB from S. aureus—S. aureus contains a second FnBP, FnBPB, which shows very significant sequence homology with FnBPA. We can use the data presented here to suggest the most likely sequence alignment of the FnBRs in the two proteins. The data that we have collected on boundary definition in both staphylococcal and streptococcal repeats argue strongly for the presence of a ^{5}F1-binding motif in FnBPA-1. This has been used to define the N-terminal boundary of the Fn-binding region of FnBPB. Both the high affinity of FnBPA-1 for Fib1 (~5 nM; Table 1) and the length of F1-binding motifs determined by our previous work (33, 37) suggest that the sequence IIQ in the N terminus of FnBPA interacts with ^{5}F1. A good match for this motif is "IIE" found in FnBPB (Fig. 6), which suggests a similar boundary for the N terminus of the Fn-binding region. Although we have yet to study Fn binding of the FnBRs from FnBPB, this observation supports the alignment of FnBRs shown in Fig. 6. Based on this alignment, we predict that FnBPB contains 10 rather than 11 FnBRs but will contain the same number (six) of high affinity binding sites for the NTD of Fn as FnBPA.

High Affinity FnBRs Harbor LIBS Epitopes for both mAbs and IgG Purified from Patient Serum—A panel of mouse mAbs was generated against full-length FnBPA and the recombinant D1–D3 sequences of FnBPA. Four of the generated monoclonal antibodies, 1F9, 5G3, 6B7, and 7D4, were further characterized. All of the mAbs appear to be LIBS antibodies in that they specifically recognize epitopes in the complex of FnBPA with Fn (50). The binding of these mAbs to the 11 FnBRs in the presence of either Fn or Fib1 was examined by an enzyme-linked immunosorbent assay (Fig. 7). As would be expected if the LIBS epitopes were generated in response to the Fib1/FnBR or Fn/FnBR complex, binding of Fn/Fib to high affinity FnBRs resulted in the highest levels of LIBS epitopes as measured by

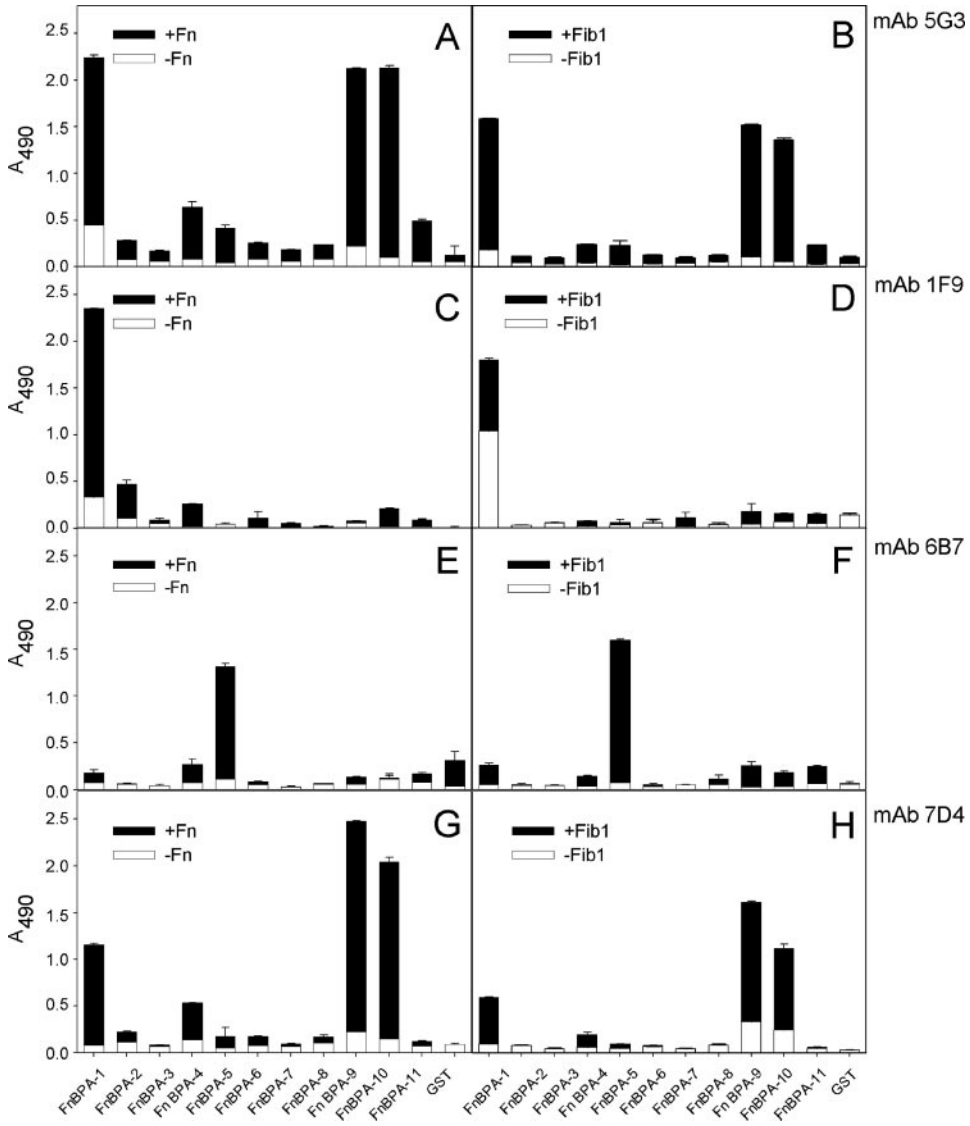

FIGURE 7. **Binding of LIBS monoclonal antibodies to high affinity FnBPA repeats.** Microtiter wells were coated with recombinant FnBRs in fusion with GST (0.5 μg in 100 μl) and incubated with 0.25 μg of the indicated anti-FnBPA LIBS monoclonal antibodies in the absence or presence of Fn (0.5 μg) or Fib1 (0.1 μg). After washing, the antibody binding was detected by incubating with a rabbit anti-mouse HRP-conjugated antibody as reported under "Experimental Procedures." *Bars* represent S.D. from means of triplicate determinations.

mAbs binding. Two mAbs (1F9 and 7D4) reacted with multiple (FnBPA-1, FnBPA-9, and FnBPA-10) FnBR-containing complexes (Fig. 7, *A*, *B*, *G*, and *H*). Given the low sequence identity between FnBPA-1 and either FnBPA-9 or FnBPA-10, this is consistent with the formation of a similar conformation in the FnBR·Fn complexes, as suggested by the tandem β-zipper model.

Samples of IgG from patients with staphylococcal infections were examined for the presence of anti-LIBS antibodies to FnBRs (Fig. 8). In the presence of Fn, the high affinity FnBRs generated the biggest response (Fig. 8*B*). In contrast, in the absence of Fn, no significant binding was observed (Fig. 8*A*). The control IgG preparations contained very low anti-LIBS activity. Taken together, these data suggest that individuals with staphylococcal infections can develop LIBS antibodies preferentially to the high affinity FnBRs from FnBPA (51). This observation underlines the *in vivo* relevance of the repeat structure defined in Fig. 1.

DISCUSSION

FnBPA, an Fn-binding MSCRAMM from *S. aureus*, was first identified in the late 1980s by Flock *et al.* (52). Subsequently, most of the Fn binding activity was localized to repeats near the C terminus of the protein (18, 44, 47, 53), but it was unclear if there was a relationship between this repeat structure and the modular structure of the NTD of Fn that had been identified as the bacterial binding site (22). More recently, additional Fn-binding sites have been identified in FnBPA (11, 47). We proposed a mechanism, the tandem β-zipper model of Fn binding to FnBPA, which specified that all binding sites could be described as being composed of a series of short motifs arranged in the correct order to bind the sequential F1 modules in the NTD of Fn. This model describes 11 potential Fn-binding sites in FnBPA that we predicted would bind with differing affinities largely dependent on the number and sequence conservation of F1-binding motifs they contain.

The results presented here show that the FnBRs bind with differing affinity to Fn and bind through the NTD. Newly defined FnBRs (FnBPA-1, -4, -5, -9, -10, and -11) bind Fn with K_D values in the nanomolar range. Thus, dissection of the FnBPA sequence into sites containing tandemly arrayed F1 module binding motifs, using the tandem β-zipper model, successfully locates high affinity binding sites. The relatively high affinity binding of FnBPA-4, which contains only three (rather than four) putative F1-binding motifs, compared with FnBPA-3 suggests the importance of the conserved residues in the ^{2}F1- and ^{4}F1-binding motifs in Fn binding. On the other hand, FnBPA-4 might bind Fib1 in a different manner. This possibility, of an alternative mechanism of binding, is supported by the stoichiometry of binding of Fib1 to FnBPA-4 (~2:1) compared with the stoichiometry of other Fib1/high affinity FnBR interactions (~1:1; Table 1).

Since FnBPA-1 is the most N-terminal of the FnBRs and FnBPA-11 is the most C-terminal, it is now clear that high affinity Fn binding occurs over a much larger region of FnBPA than had previously been considered. The demonstration that FnBPA-1 binds Fn with high affinity is also important, since this

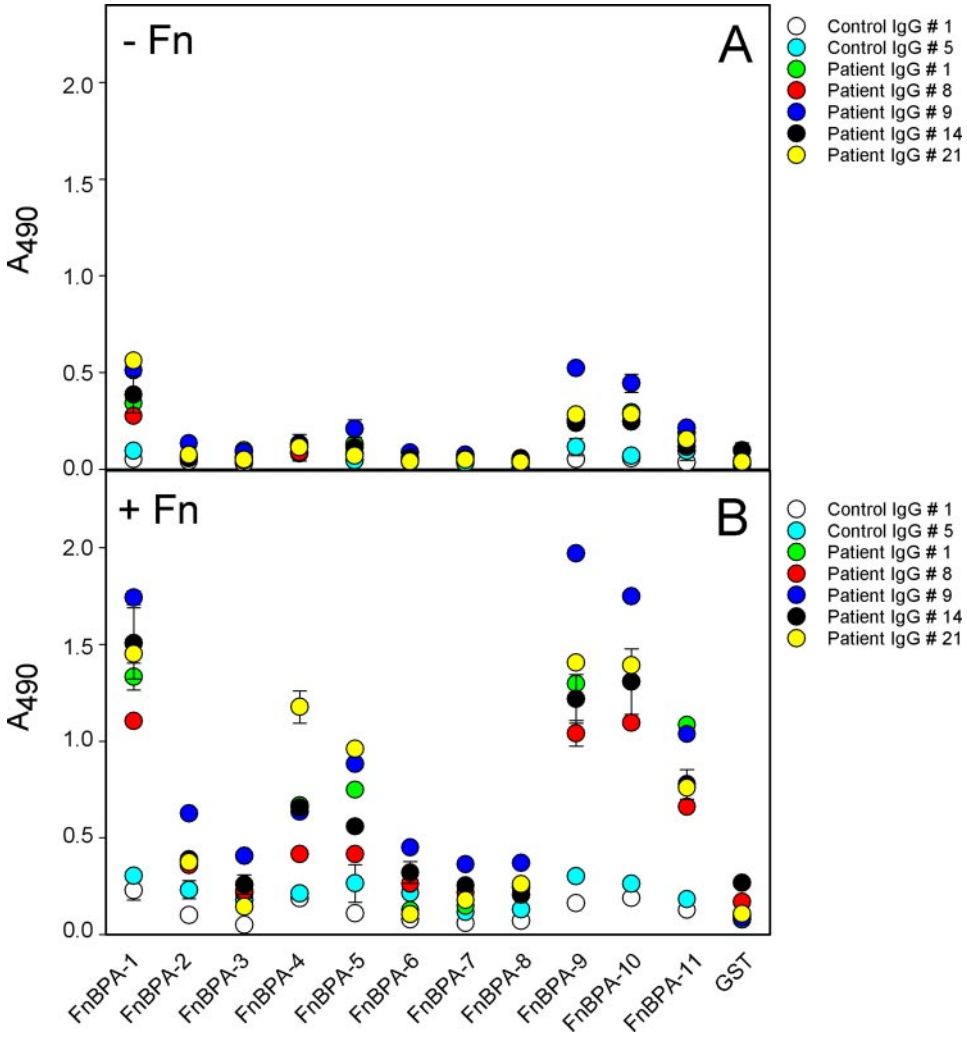

FIGURE 8. **Patients' sera contain LIBS antibodies recognize determinants in high affinity FnBPA repeats.** Microtiter wells coated with FnBPA repeats (1 μg in 100 μl) were probed with IgG isolated from sera of patients with staphylococcal infections (1 μg) in the absence (*A*) or presence (*B*) of Fn (2 μg). Bound antibody was detected by the addition of a rabbit anti-human peroxidase-conjugated IgG as reported under "Experimental Procedures." IgG from healthy donors was used as control. Data are expressed as mean ± S.D. of triplicate tests.

suggests that the A domain of FnBPA, which binds Fg (30), and the first high affinity Fn-binding site (FnBPA-1) are closer in the sequence of FnBPA than expected. It has been noted recently that Fn and Fg binding to FnBPA are both involved in activation of platelets *in vitro* and in the development of experimental endocarditis (54, 55).

IgG isolated from sera from patients with staphylococcal endocarditis reacts very weakly with FnBRs in the absence of Fn but reacts more strongly to FnBRs in the presence of Fn. This could indicate either that during staphylococcal infections the population of unbound FnBRs *in vivo* is very low (the FnBRs are mostly bound to Fn) or that antibodies to unbound FnBRs are generated less effectively than antibodies to the FnBR·Fn complex. The region of FnBPA containing FnBRs 9–11 has previously been shown to lack secondary structure (56) but to undergo a change to a more β-strand-like conformation on Fib-1 binding (53). We have previously shown that a ^{1}F1^{2}F1-binding peptide from FnBB from *S. dysgalactiae* binds largely by forming an additional antiparallel strand on the triple-stranded sheets of the sequential F1 modules (33). Thus, the formation of LIBS epitopes for mAbs and patient IgG (Figs. 7 and 8) might be consistent with this predicted unstructured-structured transition upon FnBR binding to Fn. In the presence of Fn, high affinity repeats show higher reactivity with IgG from patient sera than low affinity repeats, suggesting that the *in vitro* identification of low and high affinity FnBRs has *in vivo* relevance.

Our work here shows unequivocally that the new definition of boundaries that is involved in converting the previously defined repeats into our new functional FnBRs is critical for identifying high affinity binding sites (Fig. 5). This is the most likely explanation for the disappearance of high affinity binding sites when binding of Fn to constructs of differing length from the D region of FnBPA and FnBPB is measured (18, 44, 47). For example, FnBPA-9, -10, and -11 all bind Fib1 with K_D values in the nanomolar range, whereas D1–D3, which was defined using different boundaries, contains only two high affinity binding sites (44, 47). The difference is unlikely to arise due to a difference in fold between the two constructs, since D1–D3 has been shown to lack secondary structure prior to Fn binding (53, 56). Our model does not explain some apparent differences between the present study and a previous study of Fn binding to FnBPB (47). The work presented here, based on clearly delineated Fn-binding sites within FnBPA, represents a significant step forward in the understanding of bacterial Fn binding.

Acknowledgment—We thank Dr. S. Rindi for providing the IgG isolated from patient sera.

REFERENCES

1. Murakawa, G. J. (2004) *Cutis* **73,** (suppl.) 7–10
2. Sherwood, M., Smith, D., Crisel, R., Veledar, E., and Lerakis, S. (2006) *Am. J. Med. Sci.* **331,** 84–87
3. Ing, M. B., Baddour, L. M., and Bayers, S. A. (1997) in *The Staphylococci in Human Disease* (Crossley, K. B., and Archer, G. L., eds) pp. 331–354 Churchill Livingstone, New York
4. Davis, J. S. (2005) *Intern. Med. J.* **35,** Suppl. 2, 79–96
5. Mandal, S., Berendt, A. R., and Peacock, S. J. (2002) *J. Infect.* **44,** 143
6. Schwarz-Linek, U., Hook, M., and Potts, J. R. (2006) *Microbes Infect.* **8,** 2291–2298
7. Joh, H. J., House-Pompeo, K., Patti, J. M., Gurusiddappa, S., and Hook, M. (1994) *Biochemistry* **33,** 6086–6092

8. Fowler, T., Wann, E. R., Joh, D., Johansson, S. A., Foster, T. J., and Höök, M. (2000) *Eur. J. Cell Biol.* **79,** 672–679
9. Sinha, B., Francois, P. P., Nusse, O., Foti, M., Hartford, O. M., Vaudaux, P., Foster, T. J., Lew, D. P., Herrmann, M., and Krause, K. H. (1999) *Cell Microbiol.* **1,** 101–117
10. Peacock, S. J., Foster, T. J., Cameron, B. J., and Berendt, A. R. (1999) *Microbiology* (*Read.*) **145,** 3477–3486
11. Massey, R. C., Kantzanou, M. N., Fowler, T., Day, N. P. J., Schofield, K., Wann, E. R., Berendt, A. R., Höök, M., and Peacock, S. J. (2001) *Cell Microbiol.* **3,** 839–851
12. Kintarak, S., Whawell, S. A., Speight, P. M., Packer, S., and Nair, S. P. (2004) *Infect. Immun.* **72,** 5668–5675
13. Jett, B. D., and Gilmore, M. S. (2002) *Infect. Immun.* **70,** 4697–4700
14. Ahmed, S., Meghji, S., Williams, R. J., Henderson, B., Brock, J. H., and Nair, S. P. (2001) *Infect. Immun.* **69,** 2872–2877
15. Sinha, B., Francois, P., Que, Y. A., Hussain, M., Heilmann, C., Moreillon, P., Lew, D., Krause, K. H., Peters, G., and Herrmann, M. (2000) *Infect. Immun.* **68,** 6871–6878
16. Sinha, B., and Herrmann, M. (2005) *Thromb. Haemostasis* **94,** 266–277
17. Lowy, F. D. (2003) *J. Clin. Invest.* **111,** 1265–1273
18. Signäs, C., Raucci, G., Jonsson, K., Lindgren, P. E., Anantharamaiah, G. M., Höök, M., and Lindberg, M. (1989) *Proc. Natl. Acad. Sci. U. S. A.* **86,** 699–703
19. Talay, S. R., Valentinweigand, P., Jerlstrom, P. G., Timmis, K. N., and Chhatwal, G. S. (1992) *Infect. Immun.* **60,** 3837–3844
20. Lindgren, P. E., McGavin, M. J., Signäs, C., Guss, B., Gurusiddappa, S., Höök, M., and Lindberg, M. (1993) *Eur. J. Biochem.* **214,** 819–827
21. Probert, W. S., and Johnson, B. J. B. (1998) *Mol. Microbiol.* **30,** 1003–1015
22. Sottile, J., Schwarzbauer, J., Selegue, J., and Mosher, D. F. (1991) *J. Biol. Chem.* **266,** 12840–12843
23. Talay, S. R., Zock, A., Rohde, M., Molinari, G., Oggioni, M., Pozzi, G., Guzman, C. A., and Chhatwal, G. S. (2000) *Cell Microbiol.* **2,** 521–535
24. Raibaud, S., Schwarz-Linek, U., Kim, J. H., Jenkins, H. T., Baines, E. R., Gurusidappa, S., Hook, M., and Potts, J. R. (2005) *J. Biol. Chem.* **280,** 18803–18809
25. Nashev, D., Toshkova, K., Salasia, S. I., Hassan, A. A., Lammler, C., and Zschock, M. (2004) *FEMS Microbiol. Lett.* **233,** 45–52
26. Peacock, S. J., Day, N. P. J., Thomas, M. G., Berendt, A. R., and Foster, T. J. (2000) *J. Infect.* **41,** 23–31
27. Arrecubieta, C., Asai, T., Bayern, M., Loughman, A., Fitzgerald, J. R., Shelton, C. E., Baron, H. M., Dang, N. C., Deng, M. C., Naka, Y., Foster, T. J., and Lowy, F. D. (2006) *J. Infect. Dis.* **193,** 1109–1119
28. Rice, K., Huesca, M., Vaz, D., and McGavin, M. J. (2001) *Infect. Immun.* **69,** 3791–3799
29. Grundmeier, M., Hussain, M., Becker, P., Heilmann, C., Peters, G., and Sinha, B. (2004) *Infect. Immun.* **72,** 7155–7163
30. Wann, E. R., Gurusiddappa, S., and Hook, M. (2000) *J. Biol. Chem.* **275,** 13863–13871
31. Keane, F. M., Clarke, A. W., Foster, T. J., and Weiss, A. S. (2007) *Biochemistry* **46,** 7226–7232
32. Roche, F. M., Downer, R., Keane, F., Speziale, P., Park, P. W., and Foster, T. J. (2004) *J. Biol. Chem.* **279,** 38433–38440
33. Schwarz-Linek, U., Werner, J. M., Pickford, A. R., Gurusiddappa, S., Kim, J. H., Pilka, E. S., Briggs, J. A., Gough, T. S., Hook, M., Campbell, I. D., and Potts, J. R. (2003) *Nature* **423,** 177–181
34. Sambrook, J., Fritsch, E. F., and Maniatis, T. (1989) *Molecular cloning: A Laboratory Manual*, 2nd Ed., Cold Spring Harbor Laboratory, Cold Spring Harbor, NY
35. Chung, C. T., Niemela, S. L., and Miller, R. H. (1989) *Proc. Natl. Acad. Sci. U. S. A.* **86,** 2172–2175
36. Lofdahl, S., Guss, B., Uhlen, M., Philipson, L., and Lindberg, M. (1983) *Proc. Natl. Acad. Sci. U. S. A.* **80,** 697–701
37. Schwarz-Linek, U., Pilka, E. S., Pickford, A. R., Kim, J. H., Hook, M., Campbell, I. D., and Potts, J. R. (2004) *J. Biol. Chem.* **279,** 39017–39025
38. Vuento, M., and Vaheri, A. (1979) *Biochem. J.* **183,** 331–337
39. Zardi, L., Carnemolla, B., Balza, E., Borsi, L., Castellani, P., Rocco, M., and Siri, A. (1985) *Eur. J. Biochem.* **146,** 571–579
40. McGavin, M. J., Gurusiddappa, S., Lindgren, P. E., Lindberg, M., Raucci, G., and Höök, M. (1993) *J. Biol. Chem.* **268,** 23946–23953
41. Kohler, G., and Milstein, C. (1975) *Nature* **256,** 495–497
42. Visai, L., De Rossi, E., Valtulina, V., Casolini, F., Rindi, S., Guglierame, P., Pietrocola, G., Bellotti, V., Riccardi, G., and Speziale, P. (2003) *Biochim. Biophys. Acta* **1646,** 173–183
43. Froman, G., Switalski, L. M., Speziale, P., and Hook, M. (1987) *J. Biol. Chem.* **262,** 6564–6571
44. Huff, S., Matsuka, Y. V., McGavin, M. J., and Ingham, K. C. (1994) *J. Biol. Chem.* **269,** 15563–15570
45. Rindi, S., Cicalini, S., Pietrocola, G., Venditti, M., Festa, A., Foster, T. J., Petrosillo, N., and Speziale, P. (2006) *Eur. J. Clin. Invest.* **36,** 536–543
46. Wiseman, T., Williston, S., Brandts, J. F., and Lin, L. N. (1989) *Anal. Biochem.* **179,** 131–137
47. Ingham, K. C., Brew, S., Vaz, D., Sauder, D. N., and McGavin, M. J. (2004) *J. Biol. Chem.* **279,** 42945–42953
48. Joh, D., Speziale, P., Gurusiddappa, S., Manor, J., and Höök, M. (1998) *Eur. J. Biochem.* **258,** 897–905
49. Williams, R. J., Henderson, B., and Nair, S. P. (2002) *Calcif. Tissue Int.* **70,** 416–421
50. Speziale, P., Joh, D., Visai, L., Bozzini, S., House-Pompeo, K., Lindberg, M., and Höök, M. (1996) *J. Biol. Chem.* **271,** 1371–1378
51. Casolini, F., Visai, L., Joh, D., Conaldi, P. G., Toniolo, A., Hook, M., and Speziale, P. (1998) *Infect. Immun.* **66,** 5433–5442
52. Flock, J. I., Froman, G., Jonsson, K., Guss, B., Signäs, C., Nilsson, B., Raucci, G., Höök, M., Wadstrom, T., and Lindberg, M. (1987) *EMBO J.* **6,** 2351–2357
53. House-Pompeo, K., Xu, Y., Joh, D., Speziale, P., and Höök, M. (1996) *J. Biol. Chem.* **271,** 1379–1384
54. Que, Y.-A., Haefliger, J.-A., Piroth, L., Francois, P., Widmer, E., Entenza, J. M., Sinha, B., Herrmann, M., Francioli, P., Vaudaux, P., and Moreillon, P. (2005) *J. Exp. Med.* **201,** 1627–1635
55. Fitzgerald, J. R., Loughman, A., Keane, F., Brennan, M., Knobel, M., Higgins, J., Visai, L., Speziale, P., Cox, D., and Foster, T. J. (2006) *Mol. Microbiol.* **59,** 212–230
56. Penkett, C. J., Redfield, C., Jones, J. A., Dodd, I., Hubbard, J., Smith, R. A. G., Smith, L. J., and Dobson, C. M. (1998) *Biochemistry* **37,** 17054–17067

The Tandem β-Zipper Model Defines High Affinity Fibronectin-binding Repeats within *Staphylococcus aureus* FnBPA

Nicola A. G. Meenan, Livia Visai, Viviana Valtulina, Ulrich Schwarz-Linek, Nicole C. Norris, Sivashankarappa Gurusiddappa, Magnus Höök, Pietro Speziale and Jennifer R. Potts

J. Biol. Chem. 2007, 282:25893-25902.
doi: 10.1074/jbc.M703063200 originally published online July 2, 2007
